Electronic Research Archive

https://www.aimspress.com/journal/era

ERA, 33(8): 4763–4784.
DOI: 10.3934/era.2025214
Received: 26 June 2025
Revised: 12 August 2025
Accepted: 13 August 2025
Published: 18 August 2025

Research article

Error analysis of a high-order compact ADI scheme for 2D time-fractional convection-diffusion equation with weakly singular solutions

Jianxiong Cao*and Yuexin Xing

School of Sciences, Lanzhou University of Technology, Lanzhou 730050, China

* **Correspondence:** Email: caojianxiong2007@126.com.

Abstract: In this paper, we propose a high-order numerical method for the 2D time-fractional convection-diffusion equation with weakly singular solutions, where the time Caputo fractional derivative is approximated by using the $L2\text{-}1_\sigma$ formula on a nonuniform graded mesh, and the space derivatives are discretized by a fourth-order compact finite difference scheme on a uniform mesh. The fully discrete compact ADI scheme is established by adding a high-order term. The stability and the convergence analyses of the scheme are analyzed in L^2-norm by using the discrete energy method. It has been proved that the introduced numerical scheme has spatial fourth-order convergence, and temporal optimal $(1+\alpha)$-*th* order convergence. The numerical results show that the error estimates are sharp.

Keywords: time-fractional convection-diffusion equation; $L2\text{-}1_\sigma$ formula; ADI method; stability; convergence

1. Introduction

Fractional partial differential equations have proven effective in modeling complex systems exhibiting memory effects, non-local interactions, and anomalous transport phenomena in various scientific and engineering applications [1–3]. Among these, the time-fractional convection-diffusion (TFCD) equation has emerged as a fundamental mathematical model for characterizing critical physical processes, particularly in mass and energy transport processes, petroleum reservoir dynamics [4], and groundwater contamination studies [5]. However, since the exact solutions to TFCD equations are usually unavailable, the study of numerical methods becomes fundamentally important.

In this paper, we propose a high-order numerical scheme for the following two-dimensional (2D)

TFCD equation [6]:

$$\begin{cases} D_t^\alpha u(\mathbf{x},t) = \Delta u(\mathbf{x},t) - \nabla u(\mathbf{x},t) + f(\mathbf{x},t), & (\mathbf{x},t) \in \Omega \times (0,T], \\ u(\mathbf{x},0) = \psi_0(\mathbf{x}), & \mathbf{x} \in \Omega, \\ u(\mathbf{x},t) = 0, & (\mathbf{x},t) \in \partial\Omega \times (0,T], \end{cases} \tag{1.1}$$

where $\nabla u(\mathbf{x},t) = \left(\frac{\partial u}{\partial x}, \frac{\partial u}{\partial y}\right)^\top$ denotes the spatial gradient of u, corresponding to the convection term. $\Omega = [0,L] \times [0,L]$ denotes the spatial domain with boundary $\partial\Omega$, $\mathbf{x} = (x,y)$, $\psi_0(\mathbf{x})$ and $f(\mathbf{x},t)$ are given sufficiently smooth functions, $D_t^\alpha u(\mathbf{x},t)$ is the Caputo fractional derivative of order α with respect to t, which is defined by [1]:

$$D_t^\alpha u(\mathbf{x},t) = \frac{1}{\Gamma(1-\alpha)} \int_0^t \frac{\partial u(\mathbf{x},s)}{\partial s} \frac{ds}{(t-s)^\alpha}, \quad 0 < \alpha < 1. \tag{1.2}$$

Over the past several decades, significant advances have been made in numerical methods for TFCD equation (1.1) and their related variants. For the one-dimensional TFCD equation with smooth solutions, Cao et al. [7] developed a high-order finite difference scheme based on a uniform mesh, which achieved a temporal $(4-\alpha)$-th order convergence. Zhang et al. [6] subsequently proposed an alternative finite difference method with $(2-\alpha)$-th order convergence. The case of the one-dimensional TFCD equation with non-smooth solutions has also been studied, such as in [8], where Wang and Wen introduced a compact exponential finite difference method for multi-term time-fractional convection-reaction-diffusion problems, while Wang et al. [9] recently developed a higher-order version of this approach. Liu et al. [10] proposed a high-order compact difference method for convection-reaction-subdiffusion equation with variable exponent and coefficients. Deng et al. [11] developed a finite volume simple WENO scheme for convection-diffuiosn equation. Tiruneh et al. [12] studied the exponential fitted operator scheme for the singularly perturbed TFCD equation. For multi-dimensional problems, Ngondiep [13] established a high-order numerical method for multi-dimensional time-fractional convection-diffusion-reaction equation with a smooth solution, obtaining $(2+\alpha)$-th order temporal convergence. However, studies on multi-dimensional TFCD equations with nonsmooth solutions are still limited [14, 15]. This critical gap in the literature motivates our present investigation of high-order numerical methods for the 2D TFCD equation with a weakly singular solution.

Alternating direction implicit (ADI) structures reduce multi-dimensional problems to multiple one-dimensional problems, thus saving computational costs greatly. Roul and Rohil [14] used an compact ADI method to numerically solve the 2D TFCD equation with an initial weak singular solution. In that work, the authors used the L1 formula on graded mesh to approximate the Caputo derivative, achieving a temporal $\min\{2-\alpha, r\alpha, 2\alpha+1\}$-th order convergence, with grading parameter r. Singh and Kumar [15] recently designed a high-order compact ADI finite difference scheme for the 2D time-fractional convection-diffusion-reaction equation. They applied the $L2\text{-}1_\sigma$ formula on graded mesh to discretize the Caputo derivative, which can achieve a higher-order convergence rate in time. They also used a transformation to eliminate the convection terms when constructing a compact ADI scheme, that will simplify stability and convergence analysis. For time-fractional derivative problems, it has been pointed out in several papers (see [16] and references cited therein) that their solutions usually exhibit some initial singularities. We assume that the problem (1.1) has a unique solution that satisfies

the following regularity condition [15]:

$$\left|\frac{\partial^l u}{\partial t^l}\right| \leq C(1 + t^{\alpha-l}), \quad l = 0, 1, 2, 3. \tag{1.3}$$

In this work, we develop and analyze a new high-order compact ADI scheme for the 2D TFCD equation with a weakly singular solution. Specifically, a high-order $L2\text{-}1_\sigma$ approximation for the Caputo time fractional derivative is applied and analyzed on temporal nonuniform meshes to resolve the initial singularity. A compact finite difference approximation for spatial diffusion and convection terms is proposed, while an ADI method is applied to enhance computational efficiency. Compared to the approach in [15], our main contributions are as follows:

- Direct treatment of the original TFCD equation form without convection term elimination.

- The stability and convergence analyses of the proposed compact ADI difference method are proved by using the discrete energy method. The error estimate shows that the proposed method has spatial fourth-order convergence, and temporal optimal $(1 + \alpha)$-th order convergence.

The rest of this paper is organized as follows. Section 2 is devoted to the derivation of the fully discrete scheme. Section 3 provides a complete stability analysis of the numerical scheme using the energy method. In Section 4, we perform a detailed convergence analysis. Numerical tests are presented to validate the theoretical analysis in Section 5, along with some comparisons to existing results in [15]. Finally, Section 6 concludes the paper with a comprehensive summary of the results.

Throughout this work, we use C to denote a generic positive constant that is independent of the discretization parameters. The value of C may vary in different parts of the analysis.

2. Derivation of numerical scheme

Let N be a positive integer and define the nonuniform time nodes by $t_l = T\left(\frac{l}{N}\right)^r$ for $l = 0, 1, \ldots, N$, where r is the grading parameter. The time step size is given by $\tau_l = t_l - t_{l-1}$, and define $t_{l-1+\sigma} = t_{l-1} + \sigma\tau_l$, with $\sigma = 1 - \frac{\alpha}{2}$. For the spatial domain $\Omega = [0, L] \times [0, L]$, we consider a uniform mesh with nodes $x_i = ih_x\,(0 \leq i \leq M_1)$ and $y_j = jh_y\,(0 \leq j \leq M_2)$, where $h_x = \frac{L}{M_1}$ and $h_y = \frac{L}{M_2}$. The resulting spatial grid is denoted by $\bar{\Omega}_h = \{(x_i, y_j)|0 \leq i \leq M_1, 0 \leq j \leq M_2\}$, $\Omega_h = \bar{\Omega}_h \cap \Omega$, and $\partial\Omega_h = \bar{\Omega}_h \cap \partial\Omega$. We use $u^l_{i,j}$ and $f^l_{i,j}$ to represent the values of $u\left(x_i, y_j, t_l\right)$ and $f\left(x_i, y_j, t_l\right)$, respectively. The finite difference operators used to discretize the space derivatives are defined as:

$$\begin{aligned} \delta_x^2 u^l_{i,j} &= \frac{u^l_{i+1,j} - 2u^l_{i,j} + u^l_{i-1,j}}{h_x^2}, \quad \delta_x u^l_{i-\frac{1}{2},j} = \frac{u^l_{i,j} - u^l_{i-1,j}}{h_x}, \\ \delta_y^2 u^l_{i,j} &= \frac{u^l_{i,j+1} - 2u^l_{i,j} + u^l_{i,j-1}}{h_y^2}, \quad \delta_y u^l_{i,j-\frac{1}{2}} = \frac{u^l_{i,j} - u^l_{i,j-1}}{h_y}. \end{aligned} \tag{2.1}$$

For any grid functions $u, v \in \Omega_h$, we define the following discrete inner products and norms:

$$\begin{aligned}
&(u,v) = h_x h_y \sum_{i=1}^{M_1-1}\sum_{j=1}^{M_2-1} u_{i,j}v_{i,j}, \quad \|u\| = \sqrt{(u,u)},\\
&(\delta_x u, \delta_x v) = h_x h_y \sum_{i=1}^{M_1}\sum_{j=1}^{M_2-1} \left(\delta_x u_{i-\frac{1}{2},j}\right)\left(\delta_x v_{i-\frac{1}{2},j}\right), \quad \|\delta_x u\| = \sqrt{(\delta_x u, \delta_x u)},\\
&\left(\delta_y u, \delta_y v\right) = h_x h_y \sum_{i=1}^{M_1-1}\sum_{j=1}^{M_2} \left(\delta_y u_{i,j-\frac{1}{2}}\right)\left(\delta_y v_{i,j-\frac{1}{2}}\right), \quad \|\delta_y u\| = \sqrt{\left(\delta_y u, \delta_y u\right)}.
\end{aligned} \tag{2.2}$$

It is obvious that $\left(-\delta_x^2 u, v\right) = \left(\delta_x u, \delta_y v\right)$, $\left(-\delta_y^2 u, v\right) = \left(\delta_y u, \delta_y v\right)$.

Lemma 2.1. *From the definitions of inner product, one has*

$$(\delta_x u, u) = \left(\delta_y u, u\right) = 0. \tag{2.3}$$

Proof. Based on the definition in (2.2), we can derive:

$$\begin{aligned}
&(\delta_x u, u)\\
&\quad = h_x h_y \sum_{i=1}^{M_1-1}\sum_{j=1}^{M_2-1} \left(\delta_x u_{i,j}\right) u_{i,j}\\
&\quad = h_x h_y \sum_{j=1}^{M_2-1}\left[\sum_{i=1}^{M_1-1}\left(\frac{u_{i+1,j}-u_{i-1,j}}{2h_x}\right)u_{i,j}\right]\\
&\quad = \frac{1}{2}h_y \sum_{j=1}^{M_2-1}\left(u_{M_1,j}u_{M_1-1,j} - u_{0,j}u_{1,j}\right),
\end{aligned} \tag{2.4}$$

taking u and v vanishes on $\partial\Omega_h$ into account, one can easily obtain $(\delta_x u, u) = \left(\delta_y u, u\right) = 0$, in a similar way, we have $\left(\delta_y u, u\right) = 0$. □

Let $\mathcal{H}_2 u$ and $\mathcal{H}_1 u$ denote quadratic and linear Lagrange interpolation polynomials over $[t_{k-1}, t_k, t_{k+1}]$ and $[t_{l-1}, t_l]$, respectively. The time Caputo fractional derivative is approximated by the $L2\text{-}1_\sigma$ scheme [17, 18]:

$$\begin{aligned}
D_t^\alpha u(x,y,t)\big|_{t=t_{l-1+\sigma}} \approx D_N^\alpha u^{l-1+\sigma} &:= \frac{1}{\Gamma(1-\alpha)}\left(\sum_{k=1}^{l-1}\int_{t_{k-1}}^{t_k}\frac{\partial_s(\mathcal{H}_2 u)ds}{(t_{l-1+\sigma}-s)^\alpha} + \int_{t_{l-1}}^{t_{l-1+\sigma}}\frac{\partial_s(\mathcal{H}_1 u)ds}{(t_{l-1+\sigma}-s)^\alpha}\right)\\
&= \sum_{k=1}^{l}\mathcal{L}_{l-k}^{(l)}\delta_t u^k, \quad 1 \le l \le N,
\end{aligned} \tag{2.5}$$

where $\delta_t u_{i,j}^l = u_{i,j}^l - u_{i,j}^{l-1}$. For $l = 1$, the kernel coefficient is $\mathcal{L}_0^{(1)} = \mathcal{M}_0^1$. For $l \ge 2$, the discrete kernels $\mathcal{L}_{l-k}^{(l)}$ are defined by

$$\mathcal{L}_{l-k}^{(l)} = \begin{cases} \mathcal{M}_0^l + \rho_{l-1}\mathcal{N}_1^l, & k = l,\\ \mathcal{M}_{l-k}^l + \rho_{k-1}\mathcal{N}_{l-k+1}^l - \mathcal{N}_{l-k}^l, & 2 \le k \le l-1,\\ \mathcal{M}_{l-1}^l - \mathcal{N}_{l-1}^n, & k = 1, \end{cases} \tag{2.6}$$

where

$$\begin{aligned}
\rho_k &= \frac{\tau_k}{\tau_{k+1}}, 1 \le k \le l-1,\\
\mathcal{M}_0^l &= \frac{1}{\tau_l \Gamma(1-\alpha)} \int_{t_{l-1}}^{t_{l-\sigma}} (t_{l-1-\sigma} - s)^{-\alpha} ds = \frac{(1-\sigma)^{1-\alpha}}{\Gamma(2-\alpha)\,\tau_l^{\alpha}},\\
\mathcal{M}_{l-k}^l &= \frac{1}{\tau_k \Gamma(1-\alpha)} \int_{t_{k-1}}^{t_k} (t_{l-1-\sigma} - s)^{-\alpha} ds, \quad 1 \le k \le l-1,\\
\mathcal{N}_{l-k}^l &= \frac{2}{\tau_k (t_{k+1} - t_{k-1}) \Gamma(1-\alpha)} \int_{t_{k-1}}^{t_k} (t_{l-1-\sigma} - s)^{-\alpha} (s - t_{k-1}) ds, \quad 1 \le k \le l-1.
\end{aligned} \tag{2.7}$$

Furthermore, Eq (2.5) can be rewritten as:

$$D_t^{\alpha} u(x,y,t)\big|_{t=t_{l-1+\sigma}} = \mathcal{L}_0^{(l)} u^l - \sum_{k=0}^{l-1} \left(\mathcal{L}_{l-k-1}^{(l)} - \mathcal{L}_{l-k}^{(l)}\right) u^k + R_t^{l-1+\sigma}, \quad 1 \le l \le N, \tag{2.8}$$

where $R_t^{l-1+\sigma}$ denotes the local approximation error.

To facilitate the analysis, define a set of auxiliary discrete convolution weights. For $1 \le l \le N$, set

$$P_0^{(l)} = \frac{1}{\mathcal{L}_0^{(l)}}, \quad P_{l-k}^{(l)} = \frac{1}{\mathcal{L}_0^{(k)}} \sum_{i=k+1}^{l} \left(\frac{1}{\mathcal{L}_{i-k-1}^{(i)}} - \frac{1}{\mathcal{L}_{i-k}^{(i)}}\right) P_{l-i}^{(l)}, \quad 1 \le k \le l-1. \tag{2.9}$$

These weights satisfy the following upper bound [19]:

$$\sum_{k=1}^{l} P_{l-k}^{(l)} k^{r(\theta-\alpha)} \le \frac{11 r(1+\theta-\alpha)}{4\Gamma(1+\theta)} T^{\alpha} \left(\frac{t_l}{T}\right)^{\theta} N^{\gamma(\theta-\alpha)}, \quad \forall \theta \in (0,1). \tag{2.10}$$

In particular, letting $\theta = \alpha$ in Eq (2.10) yields a simplified estimate:

$$\sum_{k=1}^{l} P_{l-k}^{(l)} \le \frac{11}{4\Gamma(1+\alpha)} t_l^{\alpha}. \tag{2.11}$$

Lemma 2.2. *([17, 19, 20]) Let $\{v^l\}$ be a sequence of functions defined at discrete time levels. For any $l = 1, 2, \ldots, N$, the following inequalities hold:*

$$\left(D_N^{\alpha} v^{l-1+\sigma}, v^{l-1+\sigma}\right) \ge \frac{1}{2} \sum_{k=1}^{l} \mathcal{L}_{l-k}^{(l)} \left(\|v^k\|^2 - \|v^{k-1}\|^2\right) = \frac{1}{2} D_N^{\alpha} \|v^{l-1+\sigma}\|^2. \tag{2.12}$$

Lemma 2.3. *([21]) Consider the convection-diffusion equation:*

$$\begin{cases} \kappa \dfrac{d^2\phi(x)}{dx^2} - \mu \dfrac{d\phi(x)}{dx} = s(x), \quad x \in (0,H), \\ \phi(0) = \phi_0, \quad \phi(H) = \phi_H. \end{cases}$$

A fourth-order compact finite difference scheme for this problem is given by:

$$\left(\kappa + \frac{\mu^2 h^2}{12\kappa}\right) \delta_x^2 \phi_k - \mu \delta_x \phi_k = s_k + \frac{h^2}{12} \left(\delta_x^2 s_k - \frac{\mu}{\kappa} \delta_x s_k\right) + O(h^4). \tag{2.13}$$

In accordance with Lemma 2.3, let

$$\begin{aligned} \mathcal{P}_x &= 1 + \frac{h_x^2}{12}\left(\delta_x^2 - \delta_x\right), \quad \mathcal{Q}_x = -\left(1 + \frac{h_x^2}{12}\right)\delta_x^2 + \delta_x, \\ \mathcal{P}_y &= 1 + \frac{h_y^2}{12}\left(\delta_y^2 - \delta_y\right), \quad \mathcal{Q}_y = -\left(1 + \frac{h_y^2}{12}\right)\delta_y^2 + \delta_y. \end{aligned} \tag{2.14}$$

Now, by using the above compact finite difference operators to discrete the space derivative in (1.1), we obtain the following fully discrete compact difference scheme

$$D_N^{\alpha} u_{i,j}^{l-1+\sigma} + \mathcal{P}_x^{-1}\mathcal{Q}_x u_{i,j}^{l-1+\sigma} + \mathcal{P}_y^{-1}\mathcal{Q}_y u_{i,j}^{l-1+\sigma} = f_{i,j}^{l-1+\sigma} + R_t^{l-1+\sigma} + R_s^{l-1+\sigma}, \tag{2.15}$$

where $1 \le i \le M_1 - 1, 1 \le j \le M_2 - 1, 1 \le l \le N$. The initial and boundary conditions are:

$$u_{i,j}^0 = \psi_0(x_i, y_j), \quad 0 \le i \le M_1, \quad 0 \le j \le M_2 \tag{2.16}$$

$$u_{i,j}^{l-1+\sigma} = 0, \quad i = 0,\ M_1 \text{ or } j = 0,\ M_2,\ l - 1 + \sigma \ge 0. \tag{2.17}$$

Let $u_{i,j}^{l-1+\sigma} = \sigma u_{i,j}^l + (1-\sigma)u_{i,j}^{l-1} + R_1^{l-1+\sigma}$, the numerical scheme (2.15) is changed as

$$\begin{aligned} &\mathcal{L}_0^{(l)} u_{i,j}^l + \sigma\mathcal{P}_x^{-1}\mathcal{Q}_x u_{i,j}^l + \sigma\mathcal{P}_y^{-1}\mathcal{Q}_y u_{i,j}^l \\ &= \sum_{k=0}^{l-1}\left(\mathcal{L}_{l-k-1}^{(l)} - \mathcal{L}_{l-k}^{(l)}\right)u_{i,j}^k + (\sigma-1)\,\mathcal{P}_x^{-1}\mathcal{Q}_x u_{i,j}^{l-1} \\ &+ (\sigma-1)\,\mathcal{P}_y^{-1}\mathcal{Q}_y u_{i,j}^{l-1} + f_{i,j}^{l-1+\sigma} + R_t^{l-1+\sigma} + R_s^{l-1+\sigma} + R_1^{l-1+\sigma}. \end{aligned} \tag{2.18}$$

Applying the operators $P_0^{(l)}\mathcal{P}_x\mathcal{P}_y$ to both sides of (2.18), it can be reformulated as:

$$\begin{aligned} &\mathcal{P}_x\mathcal{P}_y u_{i,j}^l + \sigma P_0^{(l)}\mathcal{P}_y\mathcal{Q}_x u_{i,j}^l + \sigma P_0^{(l)}\mathcal{P}_x\mathcal{Q}_y u_{i,j}^l \\ = \;& P_0^{(l)}\mathcal{P}_x\mathcal{P}_y\left(\sum_{k=0}^{l-1}\left(\mathcal{L}_{l-k-1}^{(l)} - \mathcal{L}_{l-k}^{(l)}\right)u_{i,j}^k\right) + (\sigma-1)\,P_0^{(l)}\mathcal{P}_y\mathcal{Q}_x u_{i,j}^{l-1} + (\sigma-1)\,P_0^{(l)}\mathcal{P}_x\mathcal{Q}_y u_{i,j}^{l-1} \\ &+ P_0^{(l)}\mathcal{P}_x\mathcal{P}_y f_{i,j}^{l-1+\sigma} + P_0^{(l)}\mathcal{P}_x\mathcal{P}_y\left(R_t^{l-1+\sigma} + R_s^{l-1+\sigma} + R_1^{l-1+\sigma}\right). \end{aligned} \tag{2.19}$$

Then, set $\lambda = \sigma P_0^{(l)}$; by adding a high order term $\lambda^2\mathcal{Q}_x\mathcal{Q}_y\delta_t u_{i,j}^l$, we obtain the fully discrete compact ADI scheme for problem (1.1) as

$$\begin{aligned} &\mathcal{P}_x\mathcal{P}_y u_{i,j}^l + \sigma P_0^{(l)}\mathcal{P}_y\mathcal{Q}_x u_{i,j}^l + \sigma P_0^{(l)}\mathcal{P}_x\mathcal{Q}_y u_{i,j}^l + \lambda^2\mathcal{Q}_x\mathcal{Q}_y\delta_t u_{i,j}^l \\ = \;& P_0^{(l)}\mathcal{P}_x\mathcal{P}_y\left(\sum_{k=0}^{l-1}\left(\mathcal{L}_{l-k-1}^{(l)} - \mathcal{L}_{l-k}^{(l)}\right)u_{i,j}^k\right) + (\sigma-1)\,P_0^{(l)}\mathcal{P}_y\mathcal{Q}_x u_{i,j}^{l-1} + (\sigma-1)\,P_0^{(l)}\mathcal{P}_x\mathcal{Q}_y u_{i,j}^{l-1} \\ &+ P_0^{(l)}\mathcal{P}_x\mathcal{P}_y f_{i,j}^{l-1+\sigma} + P_0^{(l)}\mathcal{P}_x\mathcal{P}_y\left(R_t^{l-1+\sigma} + R_s^{l-1+\sigma} + R_1^{l-1+\sigma}\right) + R_2, \end{aligned} \tag{2.20}$$

where $1 \le i \le M_1 - 1, 1 \le j \le M_2 - 1, 1 \le l \le N$. The initial and boundary conditions are:

$$u_{i,j}^0 = \psi_0(x_i, y_j), \quad 0 \le i \le M_1, \quad 0 \le j \le M_2 \tag{2.21}$$

$$u_{i,j}^{l-1+\sigma} = 0, \quad i = 0,\ M_1 \text{ or } j = 0,\ M_2,\ l-1+\sigma \geq 0. \tag{2.22}$$

For $l = 1, 2, , ..., N$, Eq (2.20) can be written as

$$\begin{aligned} &\left(\mathcal{P}_x + \sigma P_0^{(l)} Q_x\right)\left(\mathcal{P}_y + \sigma P_0^{(l)} Q_y\right) u_{i,j}^{l} \\ = \ & P_0^{(l)} \mathcal{P}_x \mathcal{P}_y \left(\sum_{k=0}^{l-1} \left(\mathcal{L}_{l-k-1}^{(l)} - \mathcal{L}_{l-k}^{(l)} \right) u_{i,j}^{k} \right) + (\sigma - 1)\, P_0^{(l)} \mathcal{P}_y Q_x u_{i,j}^{l-1} + (\sigma - 1)\, P_0^{(l)} \mathcal{P}_x Q_y u_{i,j}^{l-1} \\ & + \sigma^2 \left(P_0^{(l)}\right)^2 Q_x Q_y u_{i,j}^{l-1} + P_0^{(l)} \mathcal{P}_x \mathcal{P}_y f_{i,j}^{l-1+\sigma} + \mathcal{R}, \end{aligned} \tag{2.23}$$

where $\mathcal{R} = P_0^{(l)} \mathcal{P}_x \mathcal{P}_y \left(R_t^{l-1+\sigma} + R_s^{l-1+\sigma} + R_1^{l-1+\sigma} \right) + R_2$.

By omitting the truncation error term $\mathcal{R}$, and let $\tilde{u}_{i,j}^{l}$ be the numerical approximation of $u_{i,j}^{l}$, we obtain the following numerical scheme:

$$\begin{aligned} &\left(\mathcal{P}_x + \sigma P_0^{(l)} Q_x\right)\left(\mathcal{P}_y + \sigma P_0^{(l)} Q_y\right) \tilde{u}_{i,j}^{l} \\ = \ & P_0^{(l)} \mathcal{P}_x \mathcal{P}_y \left(\sum_{k=0}^{l-1} \left(\mathcal{L}_{l-k-1}^{(l)} - \mathcal{L}_{l-k}^{(l)} \right) \tilde{u}_{i,j}^{k} \right) + (\sigma - 1)\, P_0^{(l)} \mathcal{P}_y Q_x \tilde{u}_{i,j}^{l-1} + (\sigma - 1)\, P_0^{(l)} \mathcal{P}_x Q_y \tilde{u}_{i,j}^{l-1} \\ & + \sigma^2 \left(P_0^{(l)}\right)^2 Q_x Q_y \tilde{u}_{i,j}^{l-1} + P_0^{(l)} \mathcal{P}_x \mathcal{P}_y f_{i,j}^{l-1+\sigma}. \end{aligned} \tag{2.24}$$

Further, by using the intermediate variable $u_{i,j}^{*} = \left(P_y + \sigma P_0^{(l)} Q_y\right) \tilde{u}_{i,j}^{l}$, the two-dimensional spatial problem can be transformed into two relatively easy-to-solving one-dimensional problems: Fix $j \in \{1, 2, \cdots, M_2 - 1\}$, solving

$$\begin{aligned} &\left(\mathcal{P}_x + \sigma P_0^{(l)} Q_x\right) u_{i,j}^{*} \\ =& P_0^{(l)} \mathcal{P}_x \mathcal{P}_y \left(\sum_{k=0}^{l-1} \left(\mathcal{L}_{l-k-1}^{(l)} - \mathcal{L}_{l-k}^{(l)} \right) \tilde{u}_{i,j}^{k} \right) + (\sigma - 1)\, P_0^{(l)} \mathcal{P}_y Q_x \tilde{u}_{i,j}^{l-1} + (\sigma - 1)\, P_0^{(l)} \mathcal{P}_x Q_y \tilde{u}_{i,j}^{l-1} \\ & + \sigma^2 \left(P_0^{(l)}\right)^2 Q_x Q_y \tilde{u}_{i,j}^{l-1} + P_0^{(l)} \mathcal{P}_x \mathcal{P}_y f_{i,j}^{l-1+\sigma}, \quad 1 \leq i \leq M_1 - 1, \end{aligned} \tag{2.25}$$

with

$$u_{0,j}^{*} = \left(\mathcal{P}_y + \sigma P_0^{(l)} Q_y\right) \tilde{u}_{0,j}^{l}, \quad u_{M_1,j}^{*} = \left(\mathcal{P}_y + \sigma P_0^{(l)} Q_y\right) \tilde{u}_{M_1,j}^{l}. \tag{2.26}$$

Then fix $i \in \{1, 2, \cdots, M_1 - 1\}$, solving

$$\left(\mathcal{P}_y + \sigma P_0^{(l)} Q_y\right) \tilde{u}_{i,j}^{l} = u_{i,j}^{*}, \quad 1 \leq j \leq M_2 - 1, \tag{2.27}$$

with

$$\tilde{u}_{i,0} = 0, \quad \tilde{u}_{i,M_2} = 0. \tag{2.28}$$

The coefficient matrices of (2.25) and (2.27) are both diagonally dominant, thus the fully discrete scheme (2.24) is uniquely solvable.

3. Stability analysis

Lemma 3.1. *([22], Gershgorin circle theorem) Let $A = (a_{ij}) \in \mathbb{R}^{l\times l}$. Then every eigenvalue λ of A lies within at least one Gershgorin disk*

$$D(a_{ii}, r_i) = \left\{ z \in \mathbb{C} : |z - a_{ii}| \le \sum_{j\neq i} |a_{ij}| = r_i \right\}. \tag{3.1}$$

In other words, all eigenvalues of A lie within the union of l disks centered at a_{ii} with radii r_i.

Lemma 3.2. *For the matrices associated with operators $\mathcal{P}_x$ and $\mathcal{P}_y$, their eigenvalues λ are bounded by $\frac{2}{3} \le \lambda \le 1$.*

Proof. Without loss of generality, we consider the matrix P_x corresponding to the operator $\mathcal{P}_x$. The matrix P_x is symmetric and tridiagonal. We use the symmetry properties as described in Lemma 3.1. The eigenvalue λ falls within one of the following disks:

$$\begin{aligned}
&|\lambda - \frac{10}{12}| \le \frac{1}{12}\left(1 - \frac{h_x}{2}\right),\\
&|\lambda - \frac{10}{12}| \le \frac{1}{12}\left(1 + \frac{h_x}{2}\right),\\
&|\lambda - \frac{10}{12}| \le \frac{1}{12}\left(1 - \frac{h_x}{2}\right) + \frac{1}{12}\left(1 + \frac{h_x}{2}\right) = \frac{1}{6}.
\end{aligned} \tag{3.2}$$

Consequently, the eigenvalue λ satisfies the bound $\frac{2}{3} \le \lambda \le 1$. The same result holds for $\mathcal{P}_y$ due to its similar structure. □

Lemma 3.3. *([19, 20], fractional discrete Grönwall inequality) Let $\{f^l\}_{l=1}^N$, $\{g^l\}_{l=1}^N$ and $\{\lambda_n\}_{n=0}^{N-1}$ be non-negative sequences. Suppose there exists a constant $K > 0$, independent of temporal discretization parameters, satisfying $K \ge \sum_{n=0}^{N-1} \lambda_n$, with the maximum time-step size bounded by*

$$\tau \le \tau_0 := \left(\frac{11}{2}\Gamma(2-\alpha)K\right)^{-1/\alpha}. \tag{3.3}$$

Then, for any non-negative sequence $\{w^k\}_{k=0}^N$ satisfying the discrete fractional Grönwall inequality in terms of D_N^α, which denotes the discrete approximation of the Caputo fractional derivative, the following estimate holds:

$$\sum_{k=1}^{l} \mathcal{L}_{l-k}^{(l)} \delta_t \left(w^k\right)^2 \le \sum_{k=1}^{l} \lambda_{l-k} \left(w^{k-1+\sigma}\right)^2 + w^{l-1+\sigma} f^l + \left(g^l\right)^2, \quad 1 \le l \le N. \tag{3.4}$$

Additionally, the stability estimate is given by:

$$\begin{aligned}
w^l &\le 2E_\alpha\left(\frac{11}{2}Kt_l^\alpha\right)\left(w^0 + \max_{1\le k\le l}\sum_{i=1}^{k} P_{k-i}^{(k)}(f^i + g^i) + \max_{1\le i\le l}\left\{g^i\right\}\right)\\
&\le \mathcal{K}\left(w^0 + \max_{1\le k\le l}\left\{t_{k-\sigma}^\alpha (f^k + g^k)\right\} + \max_{1\le i\le l}\left\{g^i\right\}\right)\\
&\le \mathcal{K}\left(w^0 + \max_{1\le k\le l}\left\{t_{k-\sigma}^\alpha f^k\right\} + \max_{1\le k\le l}\left\{t_{k-\sigma}^{\alpha/2} g^k\right\}\right), \quad 1 \le l \le N,
\end{aligned} \tag{3.5}$$

where $\mathcal{K}$ is a constant, and $E_\alpha(z) = \sum_{k=0}^{\infty} \frac{z^k}{\Gamma(1+k\alpha)}$ denotes the Mittag-Leffler function.

Theorem 3.4. *Suppose $\tilde{u}^l$ is the solution of* (2.15)*; then for $l = 1, 2, \ldots, N$, it satisfies*

$$\|\tilde{u}^l\| \leq C\left(\|\tilde{u}^0\| + \max_{1\leq k\leq l}\|f^k\|\right). \tag{3.6}$$

Proof. From (2.15), we have

$$D_N^\alpha \tilde{u}^{l-1+\sigma} + \mathcal{P}_x^{-1}\mathcal{Q}_x\tilde{u}^{l-1+\sigma} + \mathcal{P}_y^{-1}\mathcal{Q}_y\tilde{u}^{l-1+\sigma} = f^{l-1+\sigma}. \tag{3.7}$$

Take the discrete inner product of (3.7) with $\tilde{u}^{l-1+\sigma}$, which gives

$$\left(D_N^\alpha \tilde{u}^{l-1+\sigma}, \tilde{u}^{l-1+\sigma}\right) + \left(\mathcal{P}_x^{-1}\mathcal{Q}_x\tilde{u}^{l-1+\sigma}, \tilde{u}^{l-1+\sigma}\right) + \left(\mathcal{P}_y^{-1}\mathcal{Q}_y u^{l-1+\sigma}, \tilde{u}^{l-1+\sigma}\right) = \left(f^{l-1+\sigma}, \tilde{u}^{l-1+\sigma}\right). \tag{3.8}$$

From Lemma 2.2, we obtain:

$$\left(D_N^\alpha \tilde{u}^{l-1+\sigma}, \tilde{u}^{l-1+\sigma}\right) \geq \frac{1}{2} D_N^\alpha \|\tilde{u}^{l-1+\sigma}\|^2. \tag{3.9}$$

Considering the second term on the left-hand side (LHS) of (3.8), we substitute the operator $\mathcal{Q}_x$, then invoke (2.2) and Lemma 3.2 to derive:

$$\begin{aligned}
&\left(\mathcal{P}_x^{-1}\mathcal{Q}_x\tilde{u}^{l-1+\sigma}, \tilde{u}^{l-1+\sigma}\right)\\
=&\mathcal{P}_x^{-1}\left(-\left(1+\frac{h_x^2}{12}\right)\delta_x^2\tilde{u}^{l-1+\sigma}, \tilde{u}^{l-1+\sigma}\right)\\
=&\mathcal{P}_x^{-1}\left(1+\frac{h_x^2}{12}\right)\|\tilde{u}^{l-1+\sigma}\|_x^2\\
\geq&\left(1+\frac{h_x^2}{12}\right)\|\tilde{u}^{l-1+\sigma}\|_x^2.
\end{aligned} \tag{3.10}$$

Similarly, the third term on the LHS of (3.8) can be obtained as:

$$\left(\mathcal{P}_y^{-1}\mathcal{Q}_y\tilde{u}^{l-1+\sigma}, \tilde{u}^{l-1+\sigma}\right) \geq \left(1+\frac{h_y^2}{12}\right)\|\tilde{u}^{l-1+\sigma}\|_y^2. \tag{3.11}$$

Substituting (3.9)–(3.11) into (3.8) and applying Cauchy–Schwarz inequality, we arrive at:

$$\frac{1}{2}D_N^\alpha\|\tilde{u}^{l-1+\sigma}\|^2 + \left(1+\frac{h_x^2}{12}\right)\|\tilde{u}^{l-1+\sigma}\|_x^2 + \left(1+\frac{h_y^2}{12}\right)\|\tilde{u}^{l-1+\sigma}\|_y^2 \leq \|f^{l-1+\sigma}\| \times \|\tilde{u}^{l-1+\sigma}\|. \tag{3.12}$$

Employing the ϵ-Young inequality on the right-hand side (RHS) of (3.12), we can obtain:

$$\begin{aligned}
D_N^\alpha\|\tilde{u}^{l-1+\sigma}\|^2 &\leq C\left(\|\tilde{u}^{l-1+\sigma}\|^2 + \|f^{l-1+\sigma}\|^2\right)\\
&\leq C\left(\|\tilde{u}^{l-1+\sigma}\|^2 + \max_{1\leq k\leq l}\|f^k\|^2\right).
\end{aligned} \tag{3.13}$$

For sufficiently small $\tau \leq \tau_0$, applying Lemma 3.3, the expression can be further reduced to:

$$\|\tilde{u}^l\| \leq C\left(\|\tilde{u}^0\| + \max_{1\leq k\leq l}\|f^k\|\right). \tag{3.14}$$

The proof is now complete. □

Remark 3.5. *In this paper, the stability analysis is based on the compact difference scheme* (2.15) *by using the L^2 norm. For the stability analysis of the ADI scheme* (2.24)*, we may need to utilize other analysis techniques, such as incorporating new inner products and norms to control the extra terms, as an interesting future work.*

4. Convergence analysis

Let $e_{i,j}^l = u_{i,j}^l - \tilde{u}_{i,j}^l$ be the approximation error; thus, when $(x_i, y_j) \in \partial\Omega_h$, $e_{i,j}^l = 0$, and when $(x_i, y_j) \in \bar{\Omega}_h$, $e_{i,j}^0 = 0$. From (1.1), (2.23), and (2.24), one has the error equation:

$$\begin{aligned}
&\left(\mathcal{P}_x + \sigma P_0^{(l)} \mathcal{Q}_x\right)\left(\mathcal{P}_y + \sigma P_0^{(l)} \mathcal{Q}_y\right) e_{i,j}^l \\
=&P_0^{(l)} \mathcal{P}_x \mathcal{P}_y \left(\sum_{k=0}^{l-1} \left(\mathcal{L}_{l-k-1}^{(l)} - \mathcal{L}_{l-k}^{(l)} \right) e_{i,j}^k \right) \\
&+ (\sigma - 1)\, P_0^{(l)} \mathcal{P}_y \mathcal{Q}_x u_{i,j}^{l-1} + (\sigma - 1)\, P_0^{(l)} \mathcal{P}_x \mathcal{Q}_y e_{i,j}^{l-1} \\
&+ \sigma^2 \left(P_0^{(l)}\right)^2 \mathcal{Q}_x \mathcal{Q}_y e_{i,j}^{l-1} + \mathcal{R},
\end{aligned} \tag{4.1}$$

where $\mathcal{R} = P_0^{(l)} \mathcal{P}_x \mathcal{P}_y \left(R_t^{l-1+\sigma} + R_s^{l-1+\sigma} + R_1^{l-1+\sigma} \right) + R_2$, in which $R_t^{l-1+\sigma} := D_N^\alpha u_{i,j}^{l-1+\sigma} - D_t^\alpha u(x_i, y_j, t_{l-1+\sigma})$, $R_s^{l-1+\sigma} = O(h_x^4 + h_y^4)$, $R_1^{l-1+\sigma} := u_{i,j}^{l-1+\sigma} - \sigma u_{i,j}^l - (1-\sigma) u_{i,j}^{l-1}$, and $R_2 := \lambda^2 \mathcal{Q}_x \mathcal{Q}_y \delta_t u_{i,j}^l$.

Lemma 4.1. *Consider the inner product $\left(\mathcal{Q}_x \delta_t e^l, e^{l-1+\sigma}\right)$, we have:*

$$\left(\mathcal{Q}_x \delta_t e^l, e^{l-1+\sigma}\right) \geq -\frac{C}{2}\left(1 + \frac{h_x^2}{12}\right) \|\delta_x e^{l-1}\|^2. \tag{4.2}$$

Proof. Substituting $\mathcal{Q}_x$ into the inner product, we can obtain:

$$\begin{aligned}
&\left(\mathcal{Q}_x \delta_t e^l, e^{l-1+\sigma}\right) \\
=&-\sigma\left(1 + \frac{h_x^2}{12}\right)\left(\delta_x^2 \delta_t e^l, e^l\right) - (1-\sigma)\left(1 + \frac{h_x^2}{12}\right)\left(\delta_x^2 \delta_t e^l, e^{l-1}\right) \\
&+\sigma\left(\delta_x \delta_t e^l, e^l\right) + (1-\sigma)\left(\delta_x \delta_t e^l, e^{l-1}\right).
\end{aligned} \tag{4.3}$$

From Lemma 2.1, it follows that $\left(\delta_x e^l, e^l\right) = \left(\delta_x e^{l-1}, e^{l-1}\right) = 0$. Taking $\sigma = 1 - \alpha/2$, we then arrive at:

$$\begin{aligned}
&\left(\mathcal{Q}_x \delta_t e^l, e^{l-1+\sigma}\right) \\
=&\frac{\alpha - 1}{2}\left(1 + \frac{h_x^2}{12}\right)\left(\delta_x^2 \delta_t e^l, \delta_t e^l\right) - \frac{1}{2}\left(1 + \frac{h_x^2}{12}\right)\left(\delta_x^2 e^l + \delta_x^2 e^{l-1}, \delta_t e^l\right) + \left(\delta_x e^l, e^{l-1}\right) \\
=&\frac{1 - \alpha}{2}\left(1 + \frac{h_x^2}{12}\right)\|\delta_x \delta_t e^l\|^2 + \frac{1}{2}\left(1 + \frac{h_x^2}{12}\right)\left(\delta_x e^l + \delta_x e^{l-1}, \delta_x \delta_t e^l\right) + \left(\delta_x e^l, e^{l-1}\right).
\end{aligned} \tag{4.4}$$

It can be readily deduced that the second term on the RHS of (4.4) satisfies:

$$\begin{aligned}
&\left(\delta_x e^l + \delta_x e^{l-1}, \delta_x \delta_t e^l\right) \\
=&\left(\delta_x e^l, \delta_x e^l\right) - \left(\delta_x e^l, \delta_x e^{l-1}\right) + \left(\delta_x e^l, \delta_x e^{l-1}\right) - \left(\delta_x e^{l-1}, \delta_x e^{l-1}\right) \\
=&\|\delta_x e^l\|^2 - \|\delta_x e^{l-1}\|^2.
\end{aligned} \tag{4.5}$$

To estimate the third term on the RHS of (4.4), we employ the Cauchy–Schwarz inequality followed by the ϵ-Young inequality, yielding:

$$\left(\delta_x e^l, e^{l-1}\right) \geq -\frac{1}{2}\|\delta_x e^l\|^2 - \frac{1}{2}\|e^{l-1}\|^2 \tag{4.6}$$

Since problem (1.1) satisfies homogeneous Dirichlet boundary conditions, the discrete Poincaré inequality applies, which yields

$$\|e^{l-1}\|^2 \leq C\|\delta_x e^{l-1}\|^2. \tag{4.7}$$

Therefore, (4.4) can be simplified as:

$$\begin{aligned}
&\left(Q_x e^{l-1+\sigma}, \delta_t e^l\right) \\
\geq &\frac{1-\alpha}{2}\left(1+\frac{h_x^2}{12}\right)\|\delta_x\delta_t e^l\|^2 + \frac{1}{2}\left(1+\frac{h_x^2}{12}\right)\left(\|\delta_x e^l\|^2 - \|\delta_x e^{l-1}\|^2\right) - \frac{1}{2}\|\delta_x e^l\|^2 - \frac{1}{2}C\|\delta_x e^{l-1}\|^2 \\
\geq &-\frac{C}{2}\left(1+\frac{h_x^2}{12}\right)\|\delta_x e^{l-1}\|^2.
\end{aligned} \tag{4.8}$$

□

Lemma 4.2. *Under the regularity assumption (1.3), the truncation error R_2 satisfies*

$$\left|\frac{1}{P_0^{(l)}}R_2\right| \leq C\tau_l^{1+\alpha}\left(1 + t_{l-1}^{\alpha-1}\right). \tag{4.9}$$

Proof. Through Taylor expansion analysis under condition (1.3), we obtain the following error estimate:

$$\begin{aligned}
\left|\frac{1}{P_0^{(l)}}R_2\right| &= \left|\sigma^2 P_0^{(l)} Q_x Q_y \delta_t \tilde{u}_{i,j}^l\right| \\
&= \frac{\sigma^2}{\mathcal{M}_0^l + \rho_{l-1}\mathcal{N}_1^l}\left|Q_x Q_y \delta_t \tilde{u}_{i,j}^l\right| \\
&\leq \frac{\Gamma(2-\alpha)\,\tau_l^\alpha}{(1-\sigma)^{1-\alpha}}\sigma^2\left|Q_x Q_y\left(\tilde{u}_{i,j}^l - \tilde{u}_{i,j}^{l-1}\right)\right| \\
&\leq C\tau_l^{1+\alpha}\left(1 + t_{l-1}^{\alpha-1}\right).
\end{aligned} \tag{4.10}$$

□

Lemma 4.3. *[20, Lemma 2.2]. Let $v \in C[0,T] \cap C^2(0,T]$, and assume that $|v^{(k)}| \leq Ct^{\alpha-k}$ for $k = 0, 1, 2$ and $0 < t \leq T$. Then*

$$\|R_1^{l-1+\sigma}\| \leq CN^{-\min\{r\alpha,2\}}.$$

Lemma 4.4. *[15, 23], [20, Lemma 2.4]. Assume that $v \in C[0,T] \cap C^3(0,T]$, and $|v^{(k)}| \leq Ct^{\alpha-k}$ for $k = 0, 1, 2, 3$. Then for $1 \leq l \leq N$, it holds that*

$$\|R_t^{l-1+\sigma}\| \leq Ct_{l-1+\sigma}^{-\alpha}N^{-\min\{r\alpha,3-\alpha\}}.$$

Theorem 4.5. *Let $\tilde{u}_{i,j}^{l}$ be the numerical solution of the scheme* (2.24)*,and suppose that the exact solution of* (1.1) *satisfies the regularity condition* (1.3)*, one has*

$$\|e^{l}\| \leq C\left(N^{-min\{r\alpha,1+\alpha\}} + h_x^4 + h_y^4\right). \tag{4.11}$$

Proof. From Eqs (2.23) and (2.24), the error equation (4.1) can be changed as

$$\begin{aligned} &P_0^{(l)}\mathcal{P}_x\mathcal{P}_y D_N^{\alpha} e^{l-1+\sigma} + P_0^{(l)}\mathcal{Q}_x\mathcal{P}_y e^{l-1+\sigma} + P_0^{(l)}\mathcal{Q}_y\mathcal{P}_x e^{l-1+\sigma} + \sigma^2 (P_0^{(l)})^2 \mathcal{Q}_x\mathcal{Q}_y\delta_t e^{l} \\ &\quad = P_0^{(l)}\mathcal{P}_x\mathcal{P}_y\left(R_t^{l-1+\sigma} + R_s^{l-1+\sigma} + R_1^{l-1+\sigma}\right) + R_2. \end{aligned} \tag{4.12}$$

By definition of $R_s^{l-1+\sigma}$ and Lemma 2.3, we know that

$$|R_s^{l-1+\sigma}| \leq C(h_x^4 + h_y^4).$$

By dividing both sides of the (4.12) by $P_0^{(l)}$ and computing the inner product with $e^{l-1+\sigma}$, we obtain:

$$\begin{aligned} &\left(\mathcal{P}_x\mathcal{P}_y D_N^{\alpha} e^{l-1+\sigma}, e^{l-1+\sigma}\right) + \left(\mathcal{Q}_x\mathcal{P}_y e^{l-1+\sigma}, e^{l-1+\sigma}\right) + \left(\mathcal{Q}_y\mathcal{P}_x e^{l-1+\sigma}, e^{l-1+\sigma}\right) \\ &+ \left(\sigma^2 P_0^{(l)}\mathcal{Q}_x\mathcal{Q}_y\delta_t e^{l}, e^{l-1+\sigma}\right) = \left(\mathcal{P}_x\mathcal{P}_y\left(R_t^{l-1+\sigma} + R_s^{l-1+\sigma} + R_1^{l-1+\sigma}\right), e^{l-1+\sigma}\right) + \left(\frac{R_2}{P_0^{(l)}}, e^{l-1+\sigma}\right). \end{aligned} \tag{4.13}$$

From Lemmas 2.2 and 3.2, the first term on the LHS of (4.13) can be derived as:

$$\left(\mathcal{P}_x\mathcal{P}_y D_N^{\alpha} e^{l-1+\sigma}, e^{l-1+\sigma}\right) \geq \frac{2}{9} D_N^{\alpha}\|e^{l-1+\sigma}\|^2. \tag{4.14}$$

Based on the definitions of operators $\mathcal{Q}_x$, $\mathcal{Q}_y$, and (2.2), substituting (4.14) into (4.13), applying Lemmas 2.1 and 3.2, we derive:

$$\begin{aligned} &\frac{2}{9} D_N^{\alpha}\|e^{l-1+\sigma}\|^2 + \frac{2}{3}\left(1 + \frac{h_x^2}{12}\right)\|\delta_x e^{l-1+\sigma}\|^2 + \frac{2}{3}\left(1 + \frac{h_y^2}{12}\right)\|\delta_y e^{l-1+\sigma}\|^2 + \left(\sigma^2 P_0^{(l)}\mathcal{Q}_x\mathcal{Q}_y\delta_t e^{l}, e^{l-1+\sigma}\right) \\ &\qquad \leq \left(R_t^{l-1+\sigma} + R_s^{l-1+\sigma} + R_1^{l-1+\sigma} + \frac{R_2}{P_0^{(l)}}, e^{l-1+\sigma}\right). \end{aligned} \tag{4.15}$$

Applying Lemma 4.1 to the fourth term on the LHS of (4.15), it follows that:

$$\left(\sigma^2 P_0^{(l)}\mathcal{Q}_x\mathcal{Q}_y\delta_t e^{l}, e^{l-1+\sigma}\right) \geq -\frac{C}{2}\sigma^2 P_0^{(l)}\left(1 + \frac{h_x^2}{12}\right)\left(1 + \frac{h_y^2}{12}\right)\|\delta_x\delta_y e^{l-1}\|^2. \tag{4.16}$$

Utilizing the Cauchy–Schwarz inequality and the ϵ–Young inequality, (4.15) can be transformed as:

$$\begin{aligned} &D_N^{\alpha}\|e^{l-1+\sigma}\|^2 \\ \leq &\frac{9}{2}\left(R_t^{l-1+\sigma} + R_s^{l-1+\sigma} + R_1^{l-1+\sigma} + \frac{R_2}{P_0^{(l)}}, e^{l-1+\sigma}\right) + \frac{9}{4} C\sigma^2 P_0^{(l)}\left(1 + \frac{h_x^2}{12}\right)\left(1 + \frac{h_y^2}{12}\right)\|\delta_x\delta_y e^{l-1}\|^2 \\ \leq &\frac{9}{2}\left(\|R_t^{l-1+\sigma}\| + \|R_s^{l-1+\sigma}\| + \|R_1^{l-1+\sigma}\| + \left\|\frac{R_2}{P_0^{(l)}}\right\|\right)\|e^{l-1+\sigma}\| + \frac{9}{4} C\sigma^2 P_0^{(l)}\left(1 + \frac{h_x^2}{12}\right)\left(1 + \frac{h_y^2}{12}\right) h_x^{-2} h_y^{-2}\|e^{l-1}\|^2. \end{aligned} \tag{4.17}$$

In practice, it is reasonable to assume that both h_x and h_y have a uniform lower bound.

Now, based on the above assumption, combining Lemmas 4.2–4.4, by applying fractional discrete Grönwall inequality in Lemma 3.3, we conclude from (4.17) that:

$$\|e^l\| \leq C\left(N^{-min\{r\alpha,1+\alpha\}} + h_x^4 + h_y^4\right). \tag{4.18}$$

□

5. Numerical tests

We assume that $M_1 = M_2 = M$. To quantify the accuracy of the solution, the L^∞-norm and L^2-norm errors between the exact and numerical solutions are defined as follows:

$$E_1 = \max_{1\leq l\leq N,(x_i,y_j)\in\Omega_h} \left|\tilde{u}_{i,j}^l - u(x_i, y_j, t_l)\right|,$$
$$E_2 = \max_{1\leq l\leq N} \left\{h_x h_y \sum_{i=1}^{M_1-1}\sum_{j=1}^{M_2-1} \left|\tilde{u}_{i,j}^l - u(x_i, y_j, T)\right|^2\right\}^{1/2}.$$

The rates of convergence for spatial and temporal discretizations are determined, respectively, by:

$$Rate_1 = \frac{\log(E_1(M_1, M_2, N)) - \log(E_1(2M_1, 2M_2, N))}{\log(2)},$$
$$Rate_2 = \frac{\log(E_1(M_1, M_2, N)) - \log(E_1(2M_1, 2M_2, 2N))}{\log(2)}.$$

In this section, three numerical examples are presented to systematically verify the convergence properties of the proposed scheme. The first example considers a test problem with zero initial data and a weak singularity at $t = 0$, while the second involves a non-zero initial condition. Finally, the third example conducts a comparative analysis with existing results.

Example 1. The initial and boundary conditions of the equation are specified as follows:

$$\begin{cases} u(x, y, 0) = 0, \quad (x, y) \in (0, \pi)^2, \\ u(0, y, t) = u(\pi, y, t) = 0, \quad y \in (0, \pi), t \in (0, 1], \\ u(x, 0, t) = u(x, \pi, t) = 0, \quad x \in (0, \pi), t \in (0, 1]. \end{cases}$$

Consider the forcing function

$$f(x, y, t) = \Gamma(1 + \alpha) \sin x \sin y + t^\alpha \left[2 \sin x \sin y + \cos x \sin y + \sin x \cos y\right],$$

with the exact solution to the problem is given by $u(x, y, t) = t^\alpha \sin x \sin y$.

Tables 1–3 systematically present the computed L^∞ and L^2 error norms and their associated convergence rates across various mesh discretizations, examining three distinct values of the fractional order $\alpha \in \{0.1, 0.4, 0.7\}$ and corresponding mesh grading parameters $r \in \{1, 2/\alpha, (1 + \alpha)/\alpha\}$. The numerical evidence conclusively demonstrates that the optimal convergence behavior is attained precisely when $r = (1 + \alpha)/\alpha$, in complete agreement with the theoretically predicted convergence rates. Table 4 presents the spatial L^∞ and L^2 error norms, which numerically confirm that the proposed scheme

achieves fourth-order accuracy in spatial discretization, in excellent agreement with the theoretically predicted convergence rates.

Table 1. L^∞, L^2 errors and the convergence order with $\alpha = 0.1$ for Example 1.

r	$N = M$	L^∞ *error*	*Rate*	L^2 *error*	*Rate*
1	32	1.4183e-01		2.0646e-01	
	64	1.2311e-01	0.2042	1.7839e-01	0.2108
	128	1.0668e-01	0.2067	1.5392e-01	0.2129
	256	9.2280e-02	0.2092	1.3263e-01	0.2148
$\frac{2}{\alpha}$	32	2.2845e-02		3.2425e-02	
	64	1.1224e-02	1.0253	1.5859e-02	1.0318
	128	5.3720e-03	1.0631	7.5802e-03	1.0650
	256	2.5385e-03	1.0815	3.5800e-03	1.0823
$\frac{1+\alpha}{\alpha}$	32	1.2550e-02		1.7771e-02	
	64	5.9988e-03	1.0649	8.4634e-03	1.0702
	128	2.8290e-03	1.0844	3.9898e-03	1.0849
	256	1.3269e-03	1.0922	1.8711e-03	1.0924

Table 2. L^∞, L^2 errors and the convergence order with $\alpha = 0.4$ for Example 1.

r	$N = M$	L^∞ *error*	*Rate*	L^2 *error*	*Rate*
1	32	1.3346e-02		2.1133e-02	
	64	1.0273e-02	0.3775	1.6281e-02	0.3763
	128	8.4299e-03	0.2853	1.3249e-02	0.2973
	256	6.9719e-03	0.2740	1.0924e-02	0.2784
$\frac{2}{\alpha}$	32	8.2921e-03		1.1654e-02	
	64	3.2498e-03	1.3514	4.5603e-03	1.3536
	128	1.2524e-03	1.3757	1.7581e-03	1.3751
	256	4.7906e-04	1.3864	6.7269e-04	1.3860
$\frac{1+\alpha}{\alpha}$	32	5.2226e-03		7.3507e-03	
	64	2.0224e-03	1.3687	2.8429e-03	1.3705
	128	7.7485e-04	1.3841	1.0898e-03	1.3833
	256	2.9551e-04	1.3907	4.1577e-04	1.3902

Figure 1 illustrates the evolution of the L^∞ and L^2 errors over time for $r = 1$, $\frac{2}{\alpha}$ and $\frac{1+\alpha}{\alpha}$, where $r = 1$ corresponds to a uniform temporal mesh. It is clearly seen that graded meshes significantly improve the handling of the initial singularity and yield superior accuracy compared to the uniform mesh. The numerical results presented in Figure 1 reveal that, for small times t, the error associated with $r = \frac{2}{\alpha}$ is actually lower, particularly during the initial stage. However, as the simulation progresses, the scheme with $r = \frac{1+\alpha}{\alpha}$ demonstrates performance that is comparable to or slightly better than that with $r = \frac{2}{\alpha}$, especially in terms of stability and long-term accuracy. This suggests that choosing $r = \frac{1+\alpha}{\alpha}$ offers a better overall balance by ensuring both accuracy and theoretical optimality throughout the entire time interval, highlighting its advantage in capturing the solution's behavior more effectively over the entire

time domain.

Table 3. L^∞, L^2 errors and the convergence order with $\alpha = 0.7$ for Example 1.

r	$N = M$	L^∞ *error*	*Rate*	L^2 *error*	*Rate*
1	32	4.6850e-03		7.3445e-03	
	64	3.2184e-03	0.5417	5.0481e-03	0.5409
	128	2.1296e-03	0.5958	3.3439e-03	0.5942
	256	1.3737e-03	0.6325	2.1574e-03	0.6322
$\frac{2}{\alpha}$	32	2.0464e-03		2.8287e-03	
	64	6.4131e-04	1.6740	8.8711e-04	1.6730
	128	1.9969e-04	1.6833	2.7649e-04	1.6819
	256	6.1993e-05	1.6876	8.5895e-05	1.6866
$\frac{1+\alpha}{\alpha}$	32	1.5912e-03		2.2068e-03	
	64	4.9727e-04	1.6780	6.9017e-04	1.6769
	128	1.5468e-04	1.6847	2.1479e-04	1.6840
	256	4.7972e-05	1.6890	6.6667e-05	1.6879

Table 4. Spatial numerical results of Example 1 with $r = (1 + \alpha)/\alpha$ and $N = M^3$.

α	M	L^∞ *error*	*Rate*	L^2 *error*	*Rate*
0.5	8	9.5480e-05		1.3248e-04	
	16	5.7839e-06	4.0451	7.3154e-06	4.1787
	32	3.4490e-07	4.0677	4.2641e-07	4.1006

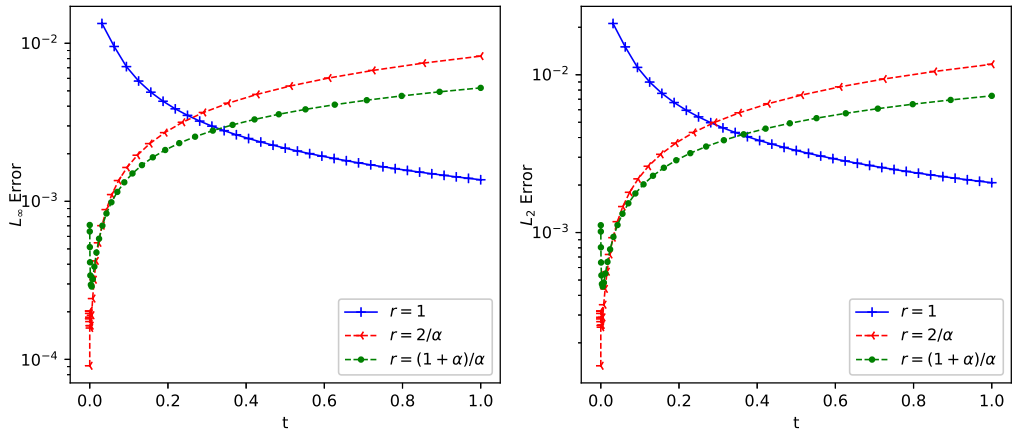

Figure 1. Evolution of L^∞ and L^2 error norms with time under different values of r with $\alpha = 0.4$, $N = M = 32$ for Example 1.

Example 2. The initial and boundary conditions for the equation are given by:

$$\begin{cases} u(x, y, 0) = e^{x+y}x(1 - x)y(1 - y), & (x, y) \in (0, 1)^2, \\ u(0, y, t) = u(1, y, t) = 0, & y \in (0, 1), t \in (0, 1], \\ u(x, 0, t) = u(x, 1, t) = 0, & x \in (0, 1), t \in (0, 1]. \end{cases}$$

The corresponding source term is given by

$$\begin{aligned} f(x,y,t) =& \Gamma(1+\alpha)(xy - x^2y - xy^2 + x^2y^2) + e^{x+y}(x + y + 4xy - x^2 - y^2 - 2x^2y - 2xy^2) \\ &+ t^{\alpha}(3x + 3y - 4xy - 3x^2 - 3y^2 + 2x^2y + 2xy^2), \end{aligned}$$

with the exact solution $u(x, y, t) = (t^{\alpha} + e^{x+y})x(1 - x)y(1 - y)$.

Table 5. L^{∞}, L^2 errors and the convergence order with $\alpha = 0.1$ for Example 2.

r	$N = M$	L^{∞} *error*	*Rate*	L^2 *error*	*Rate*
1	32	3.2896e-02		1.7690e-02	
	64	3.0093e-02	0.1285	1.6192e-02	0.1277
	128	2.7508e-02	0.1296	1.4803e-02	0.1294
	256	2.5103e-02	0.1320	1.3517e-02	0.1311
$\frac{2}{\alpha}$	32	1.1237e-02		6.1737e-03	
	64	6.1236e-03	0.8758	3.3804e-03	0.8689
	128	3.1114e-03	0.9768	1.7228e-03	0.9724
	256	1.5168e-03	1.0365	8.4113e-04	1.0344
$\frac{1+\alpha}{\alpha}$	32	7.0067e-03		3.8718e-03	
	64	3.5142e-03	0.9955	1.9478e-03	0.9912
	128	1.6999e-03	1.0477	9.4300e-04	1.0465
	256	8.0686e-04	1.0751	4.4784e-04	1.0743

Table 6. L^{∞}, L^2 errors and the convergence order with $\alpha = 0.4$ for Example 2.

r	$N = M$	L^{∞} *error*	*Rate*	L^2 *error*	*Rate*
1	32	6.0870e-03		3.3320e-03	
	64	3.6393e-03	0.7421	2.0047e-03	0.7330
	128	2.0887e-03	0.8011	1.1590e-03	0.7905
	256	1.1562e-03	0.8532	6.4625e-04	0.8427
$\frac{2}{\alpha}$	32	4.8312e-03		2.6721e-03	
	64	1.9773e-03	1.2888	1.0967e-03	1.2848
	128	7.7470e-04	1.3518	4.2995e-04	1.3509
	256	2.9765e-04	1.3800	1.652450e-04	1.3796
$\frac{1+\alpha}{\alpha}$	32	3.1350e-03		1.7380e-03	
	64	1.2375e-03	1.3410	6.8678e-04	1.3395
	128	4.7699e-04	1.3754	2.6476e-04	1.3752
	256	1.8203e-04	1.3898	1.0105e-04	1.3896

Tables 5–7 similarly present the error results and corresponding convergence rates obtained for $\alpha = 0.1, 0.4$, and 0.7 with different values of the parameter r. From these results, it is evident that the optimal convergence order of $(1 + \alpha)$ is achieved when the grading parameter is chosen as $(1 + \alpha)/\alpha$. Table 8 also presents the spatial errors and convergence rates, verifying the fourth-order accuracy in spatial discretization. These numerical findings provide rigorous validation of our theoretical analysis

and confirm the proposed method's superior computational accuracy and convergence properties under specific parameter settings.

Table 7. L^∞, L^2 errors and the convergence order with $\alpha = 0.7$ for Example 2.

r	$N = M$	L^∞ *error*	*Rate*	L^2 *error*	*Rate*
1	32	5.3277e-04		3.0170e-04	
	64	1.7896e-04	1.5739	1.0170e-04	1.5688
	128	8.2691e-05	1.1138	4.4980e-05	1.1770
	256	5.4838e-05	0.5926	2.8214e-05	0.6729
$\frac{2}{\alpha}$	32	1.3460e-03		7.4750e-04	
	64	4.2490e-04	1.6635	2.3599e-04	1.6633
	128	1.3202e-04	1.6864	7.3328e-05	1.6863
	256	4.0800e-05	1.6941	2.2659e-05	1.6943
$\frac{1+\alpha}{\alpha}$	32	1.0369e-03		5.7591e-04	
	64	3.2493e-04	1.6741	1.8044e-04	1.6743
	128	1.0070e-04	1.6901	5.5920e-05	1.6901
	256	3.1090e-05	1.6955	1.7263e-05	1.6957

Table 8. Spatial numerical results of Example 2 with $r = (1 + \alpha)/\alpha$ and $N = M^3$.

α	M	L^∞ *error*	*Rate*	L^2 *error*	*Rate*
0.5	8	3.7047e-05		2.0775e-05	
	16	1.6626e-06	4.4778	9.2840e-07	4.4839
	32	7.4704e-08	4.4761	4.1556e-08	4.4816

Similarly, Figure 2 presents the evolution of the L^∞ and L^2 errors over time for $r = 1$, $r = 2/\alpha$ and $r = (1+\alpha)/\alpha$. The results indicate that graded time meshes not only effectively reduce the numerical error, but also offer superior adaptability and robustness, particularly when handling nonsmooth solutions.

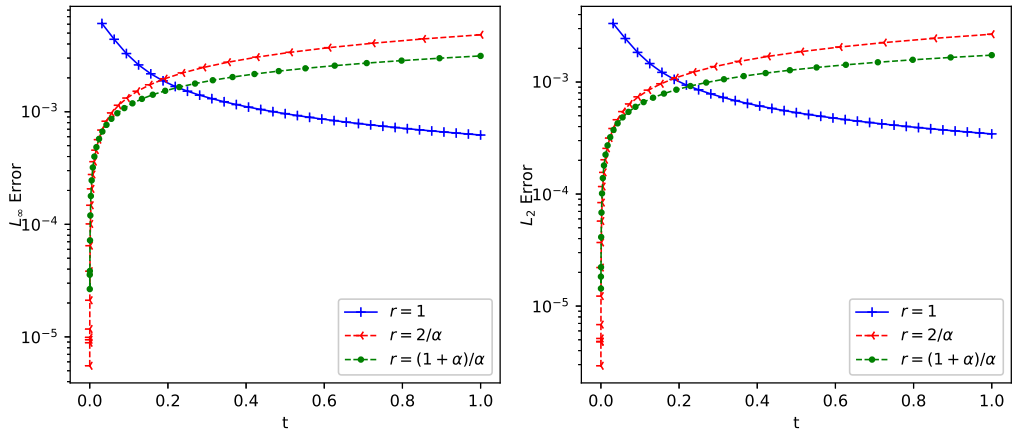

Figure 2. Evolution of L^∞ and L^2 error norms with time under different values of r with $\alpha = 0.4$, $N = M = 32$ for Example 2.

Example 3. The initial and boundary conditions are as follows:

$$\begin{cases} u(x,y,0) = 0, \quad (x,y) \in (0,\pi)^2, \\ u(0,y,t) = u(\pi,y,t) = 0, \quad y \in (0,\pi), t \in (0,1], \\ u(x,0,t) = u(x,\pi,t) = 0, \quad x \in (0,\pi), t \in (0,1]. \end{cases}$$

The forcing function is

$$f(x,y,t) = \Gamma(1+\alpha)\left(\sin x \sin y + x(\pi - x)y(\pi - y)\right) + t^{\alpha}\left(2\sin x \sin y + 2\pi(x+y) - 2(x^2+y^2)\right),$$

with the exact solution $u(x,y,t) = t^{\alpha}\left(\sin x \sin y + x(\pi - x)y(\pi - y)\right)$.

Table 9. L^{∞}, L^2 errors, and the convergence order with $\alpha = 0.1$ for Example 3.

r	$N = M$	L^{∞} *error*	*Rate*	L^2 *error*	*Rate*
1	32	7.3282e-01		1.2945e+00	
	64	6.2947e-01	0.2193	1.1151e+00	0.2152
	128	5.4024e-01	0.2205	9.5967e-01	0.2166
	256	4.6340e-01	0.2213	8.2534e-01	0.2175
$\frac{2}{\alpha}$	32	1.0987e-01		1.9680e-01	
	64	5.3486e-02	1.0386	9.5925e-02	1.0368
	128	2.5513e-02	1.0679	4.5779e-02	1.0672
	256	1.2040e-02	1.0834	2.1607e-02	1.0832
$\frac{1+\alpha}{\alpha}$	32	5.9879e-02		1.0741e-01	
	64	2.8477e-02	1.0723	5.1098e-02	1.0718
	128	1.3419e-02	1.0855	2.4079e-02	1.0855
	256	6.2925e-03	1.0926	1.1292e-02	1.0925

Table 10. L^{∞}, L^2 errors, and the convergence order with $\alpha = 0.4$ for Example 3.

r	$N = M$	L^{∞} *error*	*Rate*	L^2 *error*	*Rate*
1	32	9.4433e-02		1.5589e-01	
	64	7.5617e-02	0.3206	1.2239e-01	0.3490
	128	6.2226e-02	0.2812	9.9788e-02	0.2945
	256	5.1277e-02	0.2792	8.2080-02	0.2818
$\frac{2}{\alpha}$	32	3.8676e-02		6.9677e-02	
	64	1.5145e-02	1.3526	2.7279e-02	1.3529
	128	5.8475e-03	1.3729	1.0528e-02	1.3736
	256	2.2406e-03	1.3839	4.0327e-03	1.3844
$\frac{1+\alpha}{\alpha}$	32	2.4477e-02		4.4025e-02	
	64	9.4806e-03	1.3684	1.7045e-02	1.3690
	128	3.6400e-03	1.3810	6.5417e-03	1.3816
	256	1.3906e-03	1.3882	2.4983e-03	1.3887

Table 11. L^∞, L^2 errors, and the convergence order with $\alpha = 0.7$ for Example 3.

r	$N = M$	L^∞ *error*	*Rate*	L^2 *error*	*Rate*
1	32	3.4346e-02		5.4963e-02	
	64	2.3380e-02	0.5549	3.7761e-02	0.5416
	128	1.5360e-02	0.6061	2.5023e-02	0.5936
	256	9.8493e-03	0.6411	1.6152e-02	0.6315
$\frac{2}{\alpha}$	32	9.0906e-03		1.6561e-02	
	64	2.8562e-03	1.6703	5.2004e-03	1.6711
	128	8.9212e-04	1.6788	1.6234e-03	1.6796
	256	2.7773e-04	1.6836	5.0510e-04	1.6844
$\frac{1+\alpha}{\alpha}$	32	7.1498e-03		1.2983e-02	
	64	2.2396e-03	1.6747	4.0650e-03	1.6753
	128	6.9818e-04	1.6816	1.2666e-03	1.6823
	256	2.1705e-04	1.6856	3.9360e-04	1.6862

Table 12. Spatial numerical results of Example 3 with $r = (1 + \alpha)/\alpha$ and $N = M^3$.

α	M	L^∞ *error*	*Rate*	L^2 *error*	*Rate*
0.5	8	2.3084e-04		3.9094e-04	
	16	8.1314e-06	4.6800	1.5634e-05	4.6442
	32	2.8553e-07	4.8318	5.7716e-07	4.7596

Table 13. Comparison of L^2 errors between the proposed method and method in [15].

α	$M = N$	Present method	*Rate*	Method in [15]	*Rate*	Theoretical rate
0.2	32	8.415e-02		8.095e-02		1.2
	64	3.738e-02	1.1707	3.633e-02	1.1559	
	128	1.645e-02	1.1842	1.606e-02	1.1777	
	256	7.199e-03	1.1922	7.045e-03	1.1888	
0.4	32	4.403e-02		4.133e-02		1.4
	64	1.705e-02	1.3687	1.581e-02	1.3864	
	128	6.542e-03	1.3820	5.620e-03	1.4922	
	256	2.498e-03	1.3890	2.143e-03	1.3909	
0.6	32	2.002e-02		1.917e-02		1.6
	64	6.740e-03	1.5706	5.647e-03	1.7633	
	128	2.254e-03	1.5803	1.776e-03	1.6689	
	256	7.512e-04	1.5852	5.751e-04	1.6267	
0.8	32	8.275e-03		6.724e-03		1.8
	64	2.406e-03	1.7821	1.947e-03	1.7881	
	128	6.969e-04	1.7876	5.394e-04	1.8518	
	256	2.015e-04	1.7902	1.526e-04	1.8216	

The results for Example 4.3 are presented in Tables 9–12. Both the L^∞ and L^2 errors, along with the

temporal convergence order for different fractional orders α, are detailed in Tables 9–11. It is evident that the temporal convergence order is optimal when $r = \frac{1+\alpha}{\alpha}$. The results presented in Table 12 confirms that the discretization scheme satisfies a fourth-order spatial error convergence rate.

Additionally, Table 13 presents a comparison of the L^∞-errors between our method and that proposed in [15] for various fractional orders $\alpha = 0.2, 0.4, 0.6$, and 0.8. Although the absolute errors obtained by our method are slightly larger than those reported in [15], our approach yields convergence rates that are consistently closer to the theoretical values. This suggests that our method more accurately reflects the expected convergence behavior, demonstrating its robustness and reliability in capturing the underlying dynamics of the problem.

6. Conclusions

In this paper, we developed a high-order compact ADI finite difference scheme for the 2D time-fractional convection-diffusion equation by combining the $L2\text{-}1_\sigma$ temporal approximation with a fourth-order compact finite difference approximation of the spatial diffusion and convection operators. We then proved the unconditional stability and convergence of the scheme by applying the discrete energy method. The established numerical method has spatial fourth-order convergence, and for initially weakly singular solutions, it can achieve temporal optimal $(1 + \alpha)$-th order convergence when the temporal mesh parameter is selected properly. Comprehensive numerical experiments validate the theoretical analysis, confirming the accuracy and effectiveness of the proposed scheme.

Use of AI tools declaration

The authors declare that they have not used AI tools in preparation of this article.

Acknowledgments

This work is supported by the National Natural Science Foundation of China (NO. 12261058), Natural Science Foundation of Gansu Province under grant 22JR5RA223, Youth Doctoral Support Project of Gansu Provincial Department of Education under grant 2024QB-032 and the Hongliu Excellent Young Talents Support Program at Lanzhou University of Technology.

Conflict of interest

The authors declare that they have no conflict of interest.

References

1. I. Podlubny, *Fractional Differential Equations*, Academic Press, San Diego, 1999.
2. C. Li, F. Zeng, *Numerical Methods for Fractional Calculus*, CRC Press, Boca Raton, 2015.
3. J. Cao, W. Xu, Adaptive-coefficient finite difference frequency domain method for time fractional diffusive-viscous wave equation arising in geophysics, *Appl. Math. Lett.*, **160** (2025), 109337. https://doi.org/10.1016/j.aml.2024.109337

4. A. Chang, H. G. Sun, C. Zheng, B. Lu, C. Lu, R. Ma, et al., A time fractional convection–diffusion equation to model gas transport through heterogeneous soil and gas reservoirs, *Physica A*, **502** (2018), 356–369. https://doi.org/10.1016/j.physa.2018.02.080
5. L. Li, Z. Jiang, Z. Yin, Compact finite-difference method for 2D time-fractionalconvection–diffusion equation of groundwater pollution problems, *Comput. Appl. Math.*, **39** (2020), 142. https://doi.org/10.1007/s40314-020-01169-9
6. J. Zhang, X. Zhang, B. Yang, An approximation scheme for the time fractional convection–diffusion equation, *Appl. Math. Comput.*, **335** (2018), 305–312. https://doi.org/10.1016/j.amc.2018.04.019
7. J. Cao, C. Li, Y. Q. Chen, High-order approximation to Caputo derivatives and Caputo-type advection-diffusion equations (II), *Fract. Calc. Appl. Anal.*, **18** (2015), 735–761. https://doi.org/10.1515/fca-2015-0045
8. Y. M. Wang, X. Wen, A compact exponential difference method for multi-term time-fractional convection-reaction-diffusion problems with non-smooth solutions, *Appl. Math. Comput.*, **381** (2020), 125316. https://doi.org/10.1016/j.amc.2020.125316
9. Y. M. Wang, X. Wen, Z. Zheng, A high-order $L2\text{–}1_\sigma$ compact exponential difference method for multi-term time-fractional convection-reaction-diffusion equations, *J. Appl. Math. Comput.*, **71** (2025), 5977–6011. https://doi.org/10.1007/s12190-025-02448-6
10. M. Liu, X. Zheng, K. Li, W. Qiu, High-order compact difference method for convection-reaction–subdiffusion equation with variable exponent and coefficients, *Numer. Algorithms*, **2025** (2025). https://doi.org/10.1007/s11075-025-02060-6
11. P. Deng, G. Peng, X. Feng, D. Luo, Y. Chen, A finite volume simple WENO scheme for convection–diffusion equations, *Numer. Math. Theory Methods Appl.*, **17** (2024), 882–903. https://doi.org/10.4208/nmtma.OA-2024-0003
12. A. A. Tiruneh, H. G. Kumie, G. A. Derese, Singularly perturbed time-fractional convection–diffusion equations via exponential fitted operator scheme, *Partial Differ. Equations Appl. Math.*, **11** (2024), 100873. https://doi.org/10.1016/j.padiff.2024.100873
13. E. Ngondiep, A high-order numerical scheme for multidimensional convection-diffusion-reaction equation with time-fractional derivative, *Numer. Algorithms*, **94** (2023), 681–700. https://doi.org/10.1007/s11075-023-01516-x
14. P. Roul, V. Rohil, A high-order numerical scheme based on graded mesh and its analysis for the two-dimensional time-fractional convection-diffusion equation, *Comput. Math. Appl.*, **126** (2022), 1–13. https://doi.org/10.1016/j.camwa.2022.09.006
15. A. Singh, S. Kumar, Error analysis of a high-order fully discrete method for two-dimensional time-fractional convection-diffusion equations exhibiting weak initial singularity, *Numer. Algorithms*, **99** (2025), 251–284. https://doi.org/10.1007/s11075-024-01877-x
16. M. Stynes, E. O'Riordan, J. L. Gracia, Error analysis of a finite difference method on graded meshes for a time-fractional diffusion equation, *SIAM J. Numer. Anal.*, **55** (2017), 1057–1079. https://doi.org/10.1137/16M1082329
17. A. A. Alikhanov, A new difference scheme for the time fractional diffusion equation, *J. Comput. Phys.*, **280** (2015), 424–438. https://doi.org/10.1016/j.jcp.2014.09.031

18. C. Quan, X. Wu, Global-in-Time H^1-stability of $L2\text{-}1_\sigma$ method on general nonuniform meshes for subdiffusion equation, *J. Sci. Comput.*, **95** (2023), 59. https://doi.org/10.1007/s10915-023-02184-8

19. C. Huang, M. Stynes, A sharp α-robust $L^\infty(H^1)$ error bound for a time-fractional Allen–Cahn problem discretised by the Alikhanov $L2\text{–}1_\sigma$ scheme and a standard FEM, *J. Sci. Comput.*, **91** (2022), 43. https://doi.org/10.1007/s10915-022-01810-1

20. Z. Tan, An α-robust and new two-grid nonuniform $L2\text{–}1_\sigma$ FEM for nonlinear time-fractional diffusion equation, *Comput. Math. Appl.*, **174** (2024), 530–552. https://doi.org/10.1016/j.camwa.2024.10.023

21. A. Mohebbi, M. Abbaszadeh, Compact finite difference scheme for the solution of time fractional advection-dispersion equation, *Numer. Algorithms*, **63** (2013), 431–452. https://doi.org/10.1007/s11075-012-9631-5

22. H. Fatoorehchi, H. Abolghasemi, Finding all real roots of a polynomial by matrix algebra and the Adomian decomposition method, *J. Egypt. Math. Soc.*, **22** (2014), 524–528. https://doi.org/10.1016/j.joems.2013.12.018

23. H. Chen, M. Stynes, Error analysis of a second-order method on fitted meshes for a time-fractional diffusion problem, *J. Sci. Comput.*, **79** (2019), 624–647. https://doi.org/10.1007/s10915-018-0863-y

AIMS Press